OPEN

Citation: Transl Psychiatry (2016) 6, e724; doi:10.1038/tp.2015.211

www.nature.com/tp

ORIGINAL ARTICLE

Polymorphisms in *MIR137HG* and microRNA-137-regulated genes influence gray matter structure in schizophrenia

C Wright[1,2], CN Gupta[1], J Chen[1], V Patel[1], VD Calhoun[1,2,3], S Ehrlich[4,5,6], L Wang[7,8], JR Bustillo[2,9], NI Perrone-Bizzozero[2,9] and JA Turner[1,10]

Evidence suggests that microRNA-137 (miR-137) is involved in the genetic basis of schizophrenia. Risk variants within the miR-137 host gene (*MIR137HG)* influence structural and functional brain-imaging measures, and miR-137 itself is predicted to regulate hundreds of genes. We evaluated the influence of a *MIR137HG* risk variant (rs1625579) in combination with variants in miR-137-regulated genes *TCF4*, *PTGS2*, *MAPK1* and *MAPK3* on gray matter concentration (GMC). These genes were selected based on our previous work assessing schizophrenia risk within possible miR-137-regulated gene sets using the same cohort of subjects. A genetic risk score (GRS) was determined based on genotypes of these four schizophrenia risk-associated genes in 221 Caucasian subjects (89 schizophrenia patients and 132 controls). The effects of the rs1625579 genotype with the GRS of miR-137-regulated genes in a three-way interaction with diagnosis on GMC patterns were assessed using a multivariate analysis. We found that schizophrenia subjects homozygous for the *MIR137HG* risk allele show significant decreases in occipital, parietal and temporal lobe GMC with increasing miR-137-regulated GRS, whereas those carrying the protective minor allele show significant increases in GMC with GRS. No correlations of GMC and GRS were found in control subjects. Variants within or upstream of genes regulated by miR-137 in combination with the *MIR137HG* risk variant may influence GMC in schizophrenia-related regions in patients. Given that the genes evaluated here are involved in protein kinase A signaling, dysregulation of this pathway through alterations in miR-137 biogenesis may underlie the gray matter loss seen in the disease.

Translational Psychiatry (2016) **6,** e724; doi:10.1038/tp.2015.211; published online 2 February 2016

INTRODUCTION

MicroRNA (miRNA) are noncoding RNAs that individually regulate the expression of potentially hundreds of genes.[1] These noncoding RNAs are generally transcribed from intergenic regions; however, many are localized within introns or exons of genes called host genes.[2] After transcription, enzymes such as Drosha and the spliceosome process the primary transcript into the miRNA precursor. These miRNA precursors are then exported out of the nucleus for further processing by the enzyme Dicer into a double-stranded duplex. One or often both of these strands individually bind to Argonaute proteins and function as mature miRNAs incorporated in the miRNA-Induced Silencing Complex. In this complex, miRNAs bind to complementary sequences in target mRNAs silencing their expression by direct translational repression or mRNA degradation.[1]

Although extensive evidence supports the role of one miRNA, microRNA-137 (miR-137), in the genetic basis of schizophrenia, the mechanism of association is not known. Interest in the miRNA began after a single-nucleotide polymorphism (SNP), rs1625579, within the host gene (*MIR137HG*) was identified as the top new associated SNP in the first large schizophrenia genome-wide association study (GWAS).[3] Four other variants were identified in this GWAS within genes now experimentally verified as miR-137 targets.[4] A subsequent and larger GWAS identified another SNP near the miR-137 host gene.[5] The largest schizophrenia GWAS to date, including over 150 000 subjects, also identified a SNP, rs1702294, located closely to the previously identified rs1625579 SNP.[6] The consequences of these SNPs on miR-137 biogenesis have not yet been determined. However, post-mortem tissue analysis suggests that the rs1625579 risk genotype predicts lower miR-137 expression in the dorsolateral prefrontal cortex.[7]

Functional studies indicate that miR-137 is involved in controlling neuronal proliferation, differentiation and dendritic arborization,[8–11] all of which are important for proper neurogenesis, a process implicated in schizophrenia.[12,13] RNA expression studies suggest that miR-137 regulates expression of genes involved in schizophrenia-relevant pathways,[14] as well as neuronal differentiation.[15] Bioinformatics studies indicate that a significant number of target genes are associated with schizophrenia risk and further predict that the miRNA regulates many schizophrenia-relevant pathways.[16]

Gray matter loss is well described in schizophrenia.[17] Imaging genetics studies seek to determine how genetic factors contribute to specific regions of loss and to provide insight about how

[1]The Mind Research Network, Albuquerque, NM, USA; [2]Department of Neurosciences, University of New Mexico, Albuquerque, NM, USA; [3]Department of Electrical and Computer Engineering, University of New Mexico, Albuquerque, NM, USA; [4]Translational Developmental Neuroscience Section, Department of Child and Adolescent Psychiatry, Faculty of Medicine, Technische Universität, Dresden, Germany; [5]Department of Psychiatry, Harvard Medical School, Massachusetts General Hospital, Boston, MA, USA; [6]Athinoula A. Martinos Center for Biomedical Imaging, Massachusetts General Hospital, Charlestown, MA, USA; [7]Department of Psychiatry and Behavioral Sciences, Northwestern University Feinberg School of Medicine, Chicago, IL, USA; [8]Department of Radiology, Northwestern University Feinberg School of Medicine, Chicago, IL, USA; [9]Department of Psychiatry and Behavioral Sciences, University of New Mexico, Albuquerque, NM, USA and [10]Department of Psychology and Neuroscience Institute, Georgia State University, Atlanta, GA, USA. Correspondence: Dr NI Perrone-Bizzozero, Department of Neurosciences and Psychiatry and Behavioral Sciences, University of New Mexico School of Medicine, Albuquerque, NM 87131, USA.
E-mail: nbizzozero@salud.unm.edu
Received 7 May 2015; revised 6 October 2015; accepted 9 October 2015

plausible genetic factors may influence the pathophysiology of the disorder.[18] Studies using this approach indicate that the rs1625579 SNP influences a variety of structural and functional measures. Some effects appear to be common among risk allele carriers regardless of diagnosis,[19–21] whereas other effects appear to be unique to schizophrenia carriers.[22–25] Patients who were homozygous rs1625579 risk allele (TT) carriers in the Lett *et al.*[22] had reduced hippocampal volumes, enlarged ventricle volumes and reduced white matter integrity as compared with patients who were carriers of the protective allele (GT or GG). These protective allele carriers showed no difference from control subjects in these measures. Patel *et al.*[26] found that the hippocampal and ventricle effects of rs1625579 did not replicate in a larger sample; however, there was a consistent reduction in white matter volume in the mid-posterior corpus callosum for patients but not controls who were homozygous for the risk allele. Kelly *et al.*[23] also found that the genotype had no effect on white matter integrity measures in control subjects; moreover, a separate recent study showed a specific effect of risk alleles in miR-137 on orbital cortex–striatum white matter integrity in patients but not in controls,[27] highlighting that these effects may be related to the disease. Interestingly, at-risk subjects do appear to be influenced by this genotype in functional magnetic resonance imaging measurements of task-related brain activation. Subjects at risk for schizophrenia who were homozygous TT carriers had increased activation of the amygdala and pre- and post-central gyrus compared with GG or GT carriers, whereas the opposite genotype effect was found in controls.[24] All of these findings together suggest that that, although this variant exerts some influence across subject groups, the overall impact appears to be distinct in subjects with schizophrenia or at risk for developing the disorder. As the rs1625579 risk allele is the common allele and the disorder is thought to be polygenic in nature,[28] we propose that the variant is not influencing brain structure and function in these patients in isolation but may act in concert with other genetic and environmental factors that may contribute to schizophrenia risk as one might predict.

Given that miR-137 is known to regulate many schizophrenia-risk genes,[16] its effects on schizophrenia-related phenotypes may be modulated by genotypic variation in its target genes. We have previously demonstrated that genes regulated by miR-137 are over-represented within many schizophrenia-relevant pathways.[16] In evaluating the genetic risk within the psychiatric genomics consortium (PGC) data[3] among miR-137-regulated gene sets over-represented within these pathways, we found that several pathway-specific gene sets of miR-137-regulated genes are enriched with schizophrenia-risk variants, including genes involved in protein kinase A (PKA) signaling, long-term potentiation, axonal guidance signaling, Sertoli cell junction signaling and ephrin receptor signaling. We were able to replicate the schizophrenia-risk enrichment within the miR-137-regulated gene set involved in PKA signaling identified in the PGC data within the subjects analyzed in this study.[29] Beginning with this gene set, we have now examined the interaction of genetic variation within miR-137-regulated genes, a *MIR137HG* risk variant and schizophrenia disease status on brain measures. To our knowledge, no studies have yet evaluated the impact of the *MIR137HG* risk variant in combination with subsets of target gene variants on brain-imaging phenotypes in patients and controls.

The genes of interest included *TCF4*, *PTGS2*, *MAPK1* and *MAPK3*. *TCF4* and *PTGS2* (which encodes the COX-2 protein) are experimentally validated target genes directly regulated by this microRNA.[4,30] There is substantial evidence for TCF4 (ref. 31) in schizophrenia and, more recently, for *PTGS2*.[32,33] *MAPK1* and *MAPK3* are associated with schizophrenia[34] and are indirectly regulated by miR-137.[35–37] These genes group within the PKA-signaling pathway according to Ingenuity Pathway Analysis (Ingenuity Systems, Redwood City, CA, USA, www.ingenuity.com), and this classification is supported by experimental evidence.[38–41] The PKA signaling pathway was shown previously to be over-represented with predicted miR-137 target genes.[16]

Here we evaluated the impact of the rs1625579 genotype along with a GRC combining SNPs within and upstream of miR-137-regulated genes associated with schizophrenia risk and grouped within the PKA pathway[29] on structural patterns of gray matter concentration (GMC) loss in schizophrenia. We used independent component analyses[42–45] to avoid region-by-region or voxel-by-voxel analyses, and to reduce the number of phenotypes under consideration while capturing common patterns of GMC variation throughout the brain.

MATERIALS AND METHODS

Subject demographics

Subject imaging and genetic data were derived from the Mind Clinical Imaging Consortium (MCIC) shared repository[46] and Northwestern University (NU) data sets.[47] A total of 251 Caucasian subjects were analyzed from both data sets. After removal of subjects who did not pass quality-control filters, such as relatedness (2 subjects), genetic outliers (5 subjects), missing genotypes (13 subjects) and missing or poor image quality (10 subjects), 221 subjects remained (90 controls and 60 cases from MCIC, and 42 controls and 29 cases from NU). The schizophrenia subject cohort was identified according to the Diagnostic and Statistical Manual of Mental Disorders criteria for diagnosis of schizophrenia, schizoaffective disorder or schizophreniform disorder. See Table 1 and Supplementary Table 1 for additional subject information. All subjects provided informed consent and all subject data were collected according to the institutional review board standards and approved protocols.

Genetic data

Genotyping was performed at the Mind Research Network Neurogenetics Core lab using the Illumina Human Omni-Quad 1M BeadChip for MCIC and the Illumina Human Omni-Quad 5M chip for NU. Using PLINK (http://pngu.mgh.harvard.edu/~purcell/plink/), the genotype data from MCIC and NU were merged after updating SNP locations of MCIC to match those of the more recent NU data. Quality control was performed before and after merging with the following thresholds: Hardy–Weinberg equilibrium $P < 10^{-6}$, minor allele frequency < 0.05, missing rate per SNP < 0.02 and missing rate per individual < 0.02. Caucasian subjects were identified using the Enhancing Neuroimaging Genetics through Meta-Analysis (ENIGMA) multidimensional scaling protocol (http://enigma.ini.usc.edu/protocols/genetics-protocols/). Genetic outliers and related subjects were identified with identity-by-state and identity-by-decent testing in PLINK. One individual subject was removed from each pair or group of subjects with pi-hat values of 0.2 or greater. MCIC subjects were genotyped separately for the rs1625579 SNP at the Mind Research Network Neurogenetics Core lab using a custom TaqMan assay.

miR-137-regulated gene GRS

As noted above, we have previously found enrichment of schizophrenia-risk SNPs among several biological pathways of miR-137-regulated genes and replicated enrichment of schizophrenia-risk SNPs in PKA signaling in this cohort of subjects. This pathway contains the experimentally validated miR-137-regulated genes: *MAPK1*, *MAPK3*, *PTGS2* and *TCF4*. To assess the influence of these SNPs on GMC among these subjects, we used these SNPs to calculate a genetic risk score (GRS). Therefore, GRS was based on the variants previously identified to be the top SNPs associated with schizophrenia risk within or upstream of these miR-137-regulated genes. These SNPs were rs2276195 (*TCF4*), rs10489401 (*PTGS2*), rs9610608 (*MAPK1*) and rs7202714 (*MAPK3*). See Table 2 for additional SNP information.

The GRS was calculated across these SNPs for each subject based on the number of risk alleles (0, 1 or 2) per SNP weighted by its respective natural log-normalized (ln) odds ratio and summed for all four SNPs as was done in Walton *et al.*[48] The risk allele and odds ratio used to create GRS were derived from the PGC recent 2014 GWAS[6] (http://www.med.unc.edu/pgc/downloads). The *miR137HG* risk SNP rs1625579 genotype was not included in the PKA signaling-based risk score to allow for an analysis of the influence of this SNP on these miR-137-regulated gene variants.

Table 1. Subject demographics

Data set	*MCIC*	*NU*	*MCIC/NU merged*	*Mean age*	*Age range*	*MCIC handedness*	*MCIC mean parent SES*	*MCIC mean years of education*	*rs1625579 genotypes*
Controls	90 (61% Male)	42 (55% Male)	132 (59% Male)	32	14–60	82 Right 5 Mixed 3 Left	2.7, Range 1–5	15.3, range 12–21	TT = 87 GT = 43 GG = 2
Cases	60 (75% Male)	29 (69% Male)	89 (73% Male)	34	17–61	54 Right 4 Mixed 1 Left 1 Unknown	2.6, Range 1–5	13.6, range 7–22	TT = 63 GT = 23 GG = 3
All subjects	150 (67% Male)	71 (61% Male)	221 (65% Male)	33	21–61	136 Right 9 Mixed 4 Left 1 Unknown	2.65, Range 1–5	14.45, range 7–22	TT = 150 GT = 66 GG = 5

Abbreviations: MCIC, Mind Clinical Imaging Consortium; NU, Northwestern University; SES, socioeconomic status. Handedness, parent SES and subject years of education were only available for MCIC subjects. Parent SES was reported by 100% of controls and 95% of cases. Years of education were reported by 99% of controls and 93% of cases. Parent SES score was based on the following: 1 = situation of wealth, education, top-rank social prestige; 2 = college or advanced degree; professional or high-rank managerial position; 3 = small businessman, white-collar and skilled worker; high school graduate; 4 = semi-skilled worker, laborer; education below secondary level; 5 = unskilled and semi-skilled worker; elementary education.

Table 2. SNP information

Gene	*SNP*	*Location*	*Minor/major allele*	*Minor allele frequency in cases*	*Minor allele frequency in controls*	X^2	P-*value*	*OR for minor allele*	*PGC risk allele*	*PGC 2014 odds ratio*
MIR137HG	rs1625579	Intronic	G/T	0.163	0.178	0.1705	0.679	0.899	T	1.120
miR-137-regulated gene risk score SNPs										
TCF4	rs2276195	Intronic	T/C	0.163	0.296	10.18	0.001	0.464	T	0.990
PTGS2	rs10489401	Upstream	G/A	0.287	0.398	5.758	0.016	0.608	A	1.005
MAPK1	rs9610608	Upstream	G/A	0.191	0.102	7.037	0.008	2.073	A	0.995
MAPK3	rs7202714	Upstream	T/C	0.393	0.265	8.062	0.004	1.796	T	1.039

Abbreviations: OR, odds ratio; PGC, psychiatric genomics consortium; SNP, single-nucleotide polymorphism. Table shows information for all SNPs used in this study. All risk score SNPs were found to have significantly different minor allele frequencies between cases and controls. All SNPs are within 110 kb upstream to 40 kb downstream of each gene's boundary.

Imaging data

Structural T1 MRI scans were conducted across four sites (University of Minnesota, Massachusetts General Hospital, the University of Iowa and the University of New Mexico) for the MCIC data set and one site (NU) for the NU data set. MCIC scans were collected in the coronal orientation using Siemens (1.5 T), GE Signa (1.5 T) and Siemens Trio (3) scanners with voxel sizes of $0.625 \times 0.625 \times 1.5$, $0.664 \times 0.664 \times 1.6$ and $0.625 \times 0.625 \times 1.5$, respectively. NU scans were collected in sagittal orientation with a Siemens (1.5 T) scanner with $1 \times 1 \times 1.25$ voxel size.

Image pre-processing

All T1 Images were co-registered to the same stereotactic space using an affine transformation, resliced to $2 \times 2 \times 2$ mm and segmented into cerebrospinal fluid and gray and white matters using the Statistical Parametric Mapping 5 software (SPM5) unified segmentation method.[49] Images were visually inspected and evaluated for correlation to an averaged image across all subjects. Images with a correlation value < 0.9 to the mean image from all subjects were dropped from further analysis. Six subjects were dropped for poor image quality based on inspection and one for missing images. Three additional subjects were excluded for failing to pass the mean image correlation test. Following spatial normalization to Montreal Neurological Institute space, the images were then regressed for the effects of scanning site, gender and subject age to allow further analysis to be more sensitive to group and genotypic imaging differences. This was performed as age and gender were balanced across different sites and control/case count was balanced across sites. These regressed gray matter images were then smoothed with a full width half maximum Gaussian kernel of 10 mm. See[42,50,51] for more details on the methods used here.

Independent component analysis of imaging data

Independent component analysis (ICA) was performed on the pre-processed gray matter images. This analysis was performed using the source-based morphometry module of the GIFT toolbox (http://mialab.mrn.org/software/gift).[44] Estimation of the appropriate number of independent components to capture the variance within the subject image files was performed using a minimum description length method,[52] and was determined to be 18. We performed an ICA using the Infomax algorithm and the ICASSO algorithm 20 times with a bootstrap and random initialization each time. The imaging data were decomposed into these 18 GMC components and loading coefficients or weights respective to the contribution of each structural component to each subject's image. These loading coefficients were used to determine group contribution differences across these GMC components. The spatial maps for the components were all visually inspected, and no artifactual components were observed.

Imaging genetics statistical analysis

A multiple regression analysis was performed using the loading coefficients for the 18 independent components as dependent variables and diagnosis as the grouping factor to determine which components captured imaging variance because of the diagnostic group. Tests were deemed significant based on Bonferroni multiple testing correction

($P < 0.002$). The components that showed a significant difference between cases and controls were used in the following analyses (see Supplementary Table 3).

A multivariate analysis of covariance analysis was performed on the loading coefficients of the significant structural GMC components with the rs1625579 genotype, with chip type and diagnostic group included as factors, and the miR-137-regulated GRS included as a covariate (Supplementary Table 3). The following types of statistical analyses were considered: (1) The main effect of rs1625579 genotype, diagnosis, chip type and GRS, (2) the two-way interactions between genotype and GRS, genotype and diagnosis, GRS and diagnosis and (3) a three-way interaction between genotype, diagnosis and GRS. Given that only five subjects were homozygous for the G allele and that previous work found genotypic effects based on the analysis of collapsing the protective allele genotypes together, the rs1625579 genotype was analyzed in two groups, those homozygous for the T major allele and those having one or two of the minor allele G (GG/GT), as was performed previously.[19,22–24] Power for these analyses was calculated using G*Power 3.1.[53,54]

RESULTS

Risk score results

We have previously identified many schizophrenia-relevant pathways that were significantly enriched with miR-137-regulated genes and associated with increased schizophrenia risk.[16,29] Among these pathways, the association of schizophrenia risk with SNPs near or within miR-137-regulated genes in the PKA pathway has been replicated in the same cohort of subjects used here.[29] Therefore, these SNPs were used to calculate a GRS. Before analyzing the differences in miR-137-regulated GRS between patients and controls, we examined the distribution of these scores within each group. Using the D'Agostino–Pearson normality test,[55] which evaluates both kurtosis and skewness statistics in an omnibus test, we found that the GRS distribution for the control subjects ($z = 2.36$, P-value = 0.02) was not normal, whereas GRS among cases was normally distributed ($z = 1.34$, P-value = 0.18). Therefore, to normalize the control group scores, all scores were transformed using a negative inverse transformation (−1/(GRS+1)) in order to reduce the positive skew within the control group GRS and preserve the directionality of the risk scores. The transformed risk scores were normally distributed for both diagnostic groups (see Supplementary Figure 1 for histograms of the GRS before and after transformation). All further analyses were performed using the transformed GRS and will be further referred to simply as GRS.

The mean ± s.d. GRS for controls was -0.99 ± 0.02 and patients was -0.97 ± 0.03. Variance of GRS did not differ between the diagnostic groups using F-tests ($F(88,131) = 0.76$, $P = 0.15$), or between rs1625579 genotypic groups ($F(70,149) = 0.93$, $P = 0.70$). GRS variance was also not different between rs15625579 genotypic groups among controls only ($F(44,86) = 0.88$, $P = 0.61$) or schizophrenia subjects ($F(25,62) = 0.87$, $P = 0.64$). A Welch two-sample t-test determined that the GRS in patients were significantly greater than those in control subjects ($P = 1\text{x}10^{-4}$). GRS were not significantly different between rs1625579 genotypic groups ($P = 0.37$).

Imaging results

Among the components identified by ICA, three components had loading coefficients significantly associated with diagnostic group following Bonferroni correction for multiple comparisons (comp1: $t = -7.85$, P-value = 1.86e^{-13}, comp6: $t = -3.53$, P-value = $6\text{x}10^{-4}$ and comp 11: $t = 2.735$, P-value = $7\text{X}10^{-3}$). These components and labeled regions are shown in Figure 1, Supplementary Table 2 and Supplementary Figure 2. As expected, many brain regions showed decreased GMC in the patients, particularly in the medial frontal, temporal, inferior parietal and occipital lobes.

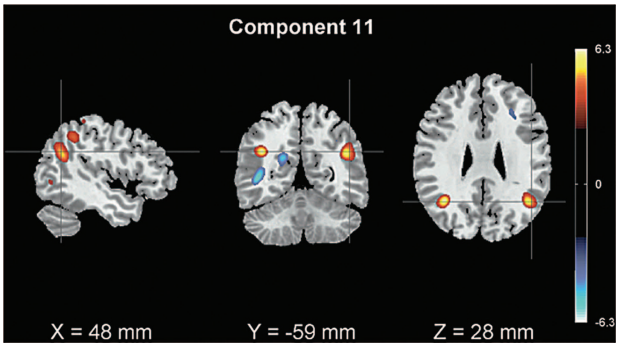

Figure 1. The spatial component showing a genetic and diagnosis-interactive effect. Regions with greater gray matter concentration (GMC) in controls than in patients include the occipital lobe (Brodmann area 19), angular gyrus (Brodmann area 39), supramarginal gyrus and the inferior parietal lobule (Brodmann area 40). The spatial map is overlaid on a template brain, thresholded with z-scores $> |3.5|$. The heat map coloring indicates z-score intensity, with red indicating findings of GMC greater in controls and blue indicating areas of GMC greater in patients. White indicates areas with greatest z-scores. z-score is indicated by the bar on the right.

Imaging genetics results

Of the three components significant for diagnosis, one (component 11) had a significant three-way interaction between the rs1625579 genotype, the miR-137-regulated GRS and diagnosis ($F(1,212) = 7.03$, P-value = 0.007, power = 0.88), which was significant following Bonferroni correction. In contrast to this three-way interaction, we found no significant main effects of the rs1625579 genotype, chip type or GRS on GMC. Variance of this component was not significantly different between diagnostic groups ($F(74,125) = 1.19$, $P = 0.40$), patient rs1625579 genotypic groups ($F(20,53) = 1.37$, $P = 0.35$) or control rs1625579 genotypic groups ($F(41,83) = 1.01$, $P = 0.96$), and the loading coefficients were normally distributed in both the controls ($z = 1.78$, P-value = 0.08) and patients ($z = -0.44$, P-value = 0.66) according to the D'Agostino test. See Supplementary Table 3 for the results from all effects and interactions. This three-way interaction was also significant when performing the analysis of variance and permuting the response variable (5000 iterations, P-value = $2.2\text{x}10^{-3}$).

Post hoc univariate analysis of the loadings for this component for the two diagnostic groups separately, and evaluating for two-way interactions between GRS and the rs1625579 genotype, revealed that the identified three-way interaction in the multivariate analysis was driven by a two-way interaction in the schizophrenia subjects alone. No significant main effect of GRS or rs1625579 genotype was found in either the control or patient group, and no significant interaction ($F(1,127) = 0.60$, P-value = 0.44) was found in the healthy control group. However, the interaction between GRS and rs1625579 genotype ($F(1,84) = 8.84$, P-value = $3.9\text{x}10^{-3}$, $\eta_p^2 = 9.52 \text{ x } 10^{-2}$, power = 0.86) was significant among the schizophrenia subjects. See Figure 2 for a graphical representation of this relationship.

To further assess this two-way interaction, a one-sided Pearson's correlation analysis was performed for both genotype groups separately. This correlation analysis demonstrated a significant negative correlation ($r(61) = -0.24$, $t = -1.9$, P-value = 0.03) between miR-137-regulated GRS and GMC loading coefficients for this component among schizophrenia patients with the TT *MiR137HG* high-risk genotype. In contrast, a significant positive correlation ($r(24) = 0.42$, $t = 2.25$, P-value = 0.02) was identified between miR-137-regulated GRS and loading coefficients among patients with the GG/GT *MiR137HG* low-risk or protective genotype. No significant correlation was identified within the

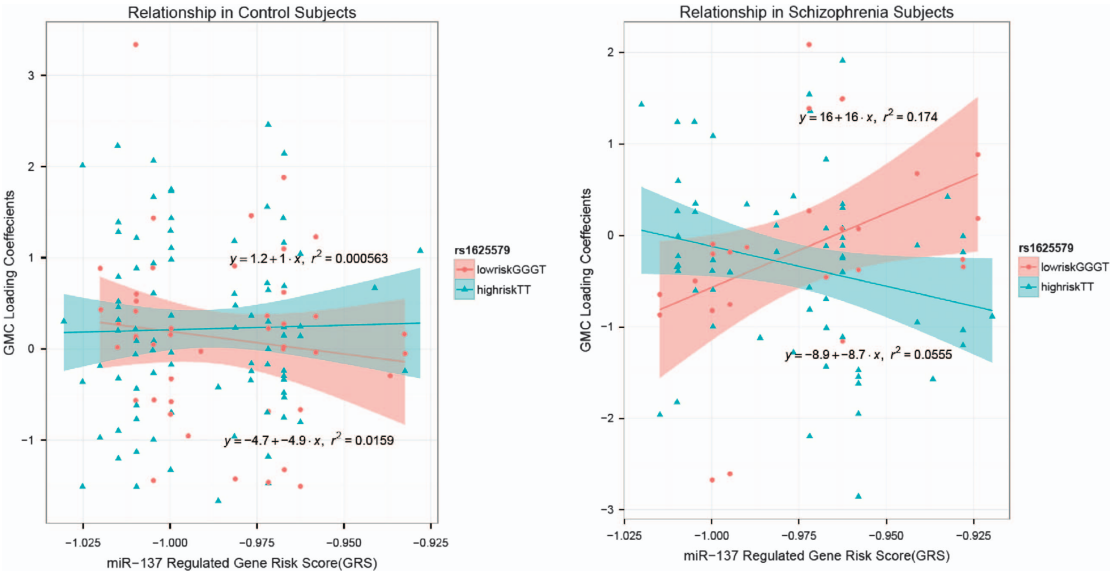

Figure 2. Relationship between gray matter concentration (GMC), diagnosis, rs1625579 genotype and miR-137-regulated genetic risk score (GRS). These graphs depict the interaction between the rs1625579 genotype and the miR-137-regulated GRS on structural loading coefficients of component 11, and the directionality of the relationship across diagnostic groups. The solid red lines indicate the best-fit trendline for subjects with the low-risk GG/GT genotype, whereas the solid blue line indicates that of the subjects with the TT or high-risk rs1625579 genotype. The area colored around the lines indicates the respective trend line s.e. The formula for each trendline is indicated on the figure nearest to the respective line. The difference in slope among the healthy control trendlines was nonsignificant ($F(1,173) = 0.19$, P-value = 0.7), whereas the difference among the schizophrenia trendlines was found to be significant ($F(1,85) = 8.95$, P-value = 3.6×10^{-3}).

control genotypic groups (high-risk *MiR137HG* genotype $r(85) = 0.02$, $t = 0.22$, P-value = 0.41, low-risk *MiR137HG* genotype $r(43) = -0.13$, $t = -0.83$, P-value = 0.21).

To assess the possibility that the influence of the GRS in the schizophrenia group was driven by one or a few of the SNPs within the risk score, further analyses of variance were performed separately, evaluating each SNP genotype weighted by the ln of the PGC odds ratio individually within the patient data. Only rs7202714 upstream of the *MAPK3* gene had a significant interaction with the rs1625579 genotype on component loadings ($F(1,83) = 9.18$, P-value = 3.3×10^{-3}) following Bonferroni correction. Additional correlation analyses were performed to evaluate this SNP among the two rs1625579 genotypic groups. One-sided Pearson's tests demonstrated that the weighted number of risk alleles for this SNP was not significantly correlated with loading coefficients in the *MIR137HG* rs1625579 high-risk TT group ($r = -0.2$, $P = 5.4 \times 10^{-2}$) but was significantly correlated among the rs1625579 low-risk GG/GT group(r) = 0.48, $P = 7 \times 10^{-3}$). Therefore, the correlation among the rs1625579 low-risk patients may be driven by this SNP; however, this does not appear to be the case for the rs1625579 high-risk patients.

The GMC spatial map for this component is shown in Figure 1 and Table 3, with the greatest weightings in the spatial map being in the occipital lobe and regions of the parietal and temporal lobes. The findings include previously well-known schizophrenia-relevant regions including the angular gyrus (Brodmann area 39), the supramarginal gyrus and the inferior parietal lobule (Brodmann area 40). Supplementary Figure 2 depicts the areas of GMC variance captured by the other two components. Figure 2 shows the relationship between the rs1625579 genotype and the genetic risk for the associated component with GMC loading coefficients for both diagnostic groups. Overall, our results indicate that the increased genetic risk by the *MIR137HG* genotype and regulated gene risk genotypes (GRS) is associated with GMC reductions in subjects with schizophrenia but not in controls. Among these patients the rs1625579 genotype appears to determine the direction of the influence of GRS on GMC.

DISCUSSION

Our results indicate a schizophrenia-specific interaction of the rs1625579 genotype with cumulative risk summed across a subset of miR-137-regulated risk gene SNPs. The interaction of this genotype with the miR-137-regulated GRS is associated with reduced GMC within the occipital, parietal and temporal lobes. Within patients with schizophrenia, those with two risk alleles (TT) showed decreasing GMC in these regions with increasing GRS, whereas those with only a single or no risk allele showed increasing GMC with increasing GRS. This suggests that the miR-137-regulated gene risk may actually be protective in the absence of the miR-137-associated risk genotype, further emphasizing the importance of evaluating the combined influence of risk genotypes. This pattern was not present in healthy controls, and if anything was reversed (although not significantly). This is in agreement with previous findings,[22–25] demonstrating that this variant may exert some influence on brain structure and function in a manner unique to schizophrenia subjects, and provides further evidence that some effects of the variant may be dependent or modulated by other genetic factors such as the risk SNPs within these miR-137-regulated genes studied here. This finding may be indicative of a complex and interactive genetic architecture where the same networks of genes influence endophenotypes in patients and controls in distinct ways. Supporting this idea, a recent study suggests that the hidden heritability underlying the polygenic risk of schizophrenia may be mediated by complex gene–gene interactive networks that are associated with distinct endophenotypes.[56] Genes that show limited significance for genetic risk in GWAS may have a robust cumulative influence on endophenotypes, as has been demonstrated for dorsolateral prefrontal cortex inefficiency, a well-established schizophrenia-associated intermediate phenotype.[57] Recent research suggests that the combined methylation status of hsa-miR219a-5p target genes is correlated with hippocampal volume, another schizophrenia-related endophenotype, further implicating a role of miRNA regulation in choreographing complex genetic influence on schizophrenia-associated endophenotypes.[58]

Table 3. Brain regions in the spatial pattern that showed genetic and diagnostic interactive effects

Spatial weighting	*Area*	*L/R Brodmann area*	*L/R volume (cm^3)*	*L/R max Z-score region and coordinates (x, y, z)*
Positively weighted	Inferior occipital gyrus/inferior parietal lobule	19/40	0.8/0.6	6.4 (−38, −68, 2)/5.2 (36, −41, 37)
	Angular gyrus	39/39	0.4/0.8	6.3 (−40, −55, 29)/5.9 (44, −55, 27)
	Middle occipital gyrus	19/NA	1.0/0.0	5.8 (−40, −70, 5)/NA
	Occipital gyrus/inferior temporal gyrus	19/47	0.4/0.3	5.8 (−42, −70, 2)/4.7 (42, −66, 2)
	Angular gyrus/inferior parietal lobule	39/40	0.4/1.5	5.3 (−40, −51, 27)/5.7 (40, −41, 37)
	Angular gyrus	39/39	0.3/0.5	4.7 (−40, −55, 32)/5.4 (44, −57, 30)
	Inferior parietal lobule, supramarginal gyrus	NA/40	0.0/1.3	NA/5.3 (44, −43, 39)
	Middle temporal gyrus	39/39	0.3/0.3	5.1 (−40, −59, 29)/4.6 (46, −57, 23)
	Fusiform gyrus	19/NA	0.1/0.0	4.3 (−40, −70, −5)/NA
	Superior parietal lobule	7/7	0.1/0.4	3.8 (−34, −65, 51)/4.3 (32, −67, 49)
	Calcarine/lingual gyrus	18/18	0.2/0.1	3.8 (−6, −95, −5)/3.6 (20, −82, −1)
Negatively weighted	Middle occipital gyrus	18/NA	0.7/0.0	5.8 (−30, −77, 13)/NA
	Middle temporal gyrus	37/NA	0.8/0.0	5.7 (−44, −56, 5)/NA
	Cuneus	23/48	1.0/0.6	4.9 (−18, −55, 25)/4.4 (34, 15, 29)
	Middle frontal gyrus	NA/48	0.0/0.4	NA/4.1 (30, 27, 26)
	Inferior temporal gyrus	20/NA	0.3/0.0	4.1 (−46, −23, −24)/NA
	Precuneus	23/NA	0.1/0.0	3.9 (−14, −52, 17)/NA
	Lingual gyrus	18/18	0.1/0.1	3.8 (−18, −72, 2)/3.8 (16, −70, 3)

Abbreviations: GMC, gray matter concentration; L, left; NA, Not applicable; R, right. Table shows the brain regions of GMC variance between patients and controls for component 11. Findings are shown for the L and R.

Given the role of the genes studied here in the PKA pathway, our results suggest that, within schizophrenia, the rs1625579 *MIR137HG* SNP in conjunction with specific genotypes within the PKA pathway may cause altered regulation of the genes within our risk score, leading to decreased GMC within Brodmann area 19 of the occipital lobe, Brodmann area 39 of the angular gyrus and Brodmann area 40 of the supramarginal gyrus and inferior parietal lobule. These regions have all previously been implicated in schizophrenia and are associated with exploratory eye movement dysfunction,[59] theory of mind or self-sensing deficits,[60] hallucinations,[61–64] adaptive control deficits[65] and attention deficits.[66,67] In addition, these regions are involved in visual processing, which is disrupted in schizophrenia.[68] The evaluated miR-137-regulated genes and PKA signaling pathway appear to be critical for proper maturation of visual processing systems.[69] This raises promising possibilities that these genetic variations within people with schizophrenia could be related to GMC and functional loss within these networks, leading to previously unexplained variation in clinical symptoms and capabilities.

Interestingly, a risk genotype for a variant within another miR-137 experimentally validated target gene, *CACNA1C*, was associated with reduced activity in Brodmann area 40 during orientation of attention in a functional magnetic resonance imaging study.[66] Gray matter volume decrease of the supramarginal gyrus was also associated with poor cognitive test scores in unaffected relatives of schizophrenia patients, further suggesting genetic liability of alterations in this region.[70] The 22q.11.2 deletion, one of the highest known risk factors for schizophrenia, is associated with altered miRNA biogenesis[71] and cortical morphological reduction of this region.[72] The effect of the *MIR137HG* risk SNPs on the biogenesis of the miRNA has not been determined; however, a recent study indicates that major alleles in these SNPs including the risk T allele of rs1625579 results in lower levels of mature miR-137 than those with the minor and protective G allele.[73] Furthermore, a post-mortem tissue analysis[7] also suggests that the biogenesis of this miRNA may be disrupted in carriers of the rs1625579 risk genotype. Therefore, other findings implicating this region in schizophrenia may be caused in part by a reduction in miR-137.

Very few studies have evaluated the role of PKA signaling on GMC in the brain regions implicated here. However, it is clear that this signaling pathway[74] and each of the investigated genes are associated with schizophrenia.[31–34] Further research will be required to determine the exact mechanism of the association presented in this study, evaluate the replicability of these findings in other cohorts and determine whether these genetic factors also influence exploratory eye movement, self-sensing, hallucinations, adaptive control or attention characteristics. One important limitation of our study is the fact that subjects were scanned at multiple sites with different scanners, increasing intersubject variability and possibly lowering the power. However, our research suggests that our method of regressing site and scanner effects from the images during pre-processing can lead to reproducible results across multiple sites of data found within well-powered single sites alone.[51] In addition, we cannot decipher the influence of antipsychotic medication usage and disease status on the GMC measures in the schizophrenia subjects, as medication information was not available for every subject. Indeed, it is possible that these genetic variants may influence the severity of such medication influence on gray matter. More research is required to tease apart the influence of the variants and medication use on GMC and to investigate the influence of other variants in miR-137-regulated genes. Nonetheless, our analysis is a first step into determining the combined effect of *MIR137HG* risk SNPs with miR-137-regulated gene variants on gray matter structure. Our results suggest that key schizophrenia regions, previously implicated in both structural and functional brain-imaging studies, are affected by rs1625579 vulnerability.

CONFLICT OF INTEREST

The authors declare no conflict of interest.

ACKNOWLEDGMENTS

This work was supported by The National Institutes of Health (5R01MH094524-03 to VDC and JAT). The MCIC data set was collected through support from the Department of Energy (DE-FG02-99ER62764 to VDC) and the National Institutes of Health (5P20RR021938/P20GM103472 and R01EB005846 to VDC). The NU data set was shared through support from the National Institutes of Health grants (P50 MH071616, R01 MH056584, 1R01 MH084803 to LW) and 1U01 MH097435 (LW and JAT). We thank the participants who enrolled in the studies used in this analysis, as well as Marilee Morgan for assistance with genotyping.

REFERENCES

1 Bartel DP. MicroRNAs: target recognition and regulatory functions. *Cell* 2009; **136**: 215–233.
2 Rodriguez A, Griffiths-Jones S, Ashurst JL, Bradley A. Identification of mammalian microRNA host genes and transcription units. *Genome Res* 2004; **14**: 1902–1910.
3 Ripke S, Sanders AR, Kendler KS, Levinson DF, Sklar P, Holmans PA *et al.* Genome-wide association study identifies five new schizophrenia loci. *Nat Genet* 2011; **43**: 969–976.
4 Kwon E, Wang W, Tsai L-H. Validation of schizophrenia-associated genes CSMD1, C10orf26, CACNA1C and TCF4 as miR-137 targets. *Mol Psychiatry* 2013; **18**: 11–12.
5 Ripke S, O'Dushlaine C, Chambert K, Moran JL, Kähler AK, Akterin S *et al.* Genome-wide association analysis identifies 13 new risk loci for schizophrenia. *Nat Genet* 2013; **45**: 1150–1159.
6 Ripke S, Neale BM, Corvin A, Walters JTR, Farh K-H, Holmans PA *et al.* Biological insights from 108 schizophrenia-associated genetic loci. *Nature* 2014; **511**: 421–427.
7 Guella I, Sequeira A, Rollins B, Morgan L, Torri F, van Erp TGM *et al.* Analysis of miR-137 expression and rs1625579 in dorsolateral prefrontal cortex. *J Psychiatr Res* 2013; **47**: 1215–1221.
8 Silber J, Lim DA, Petritsch C, Persson AI, Maunakea AK, Yu M *et al.* miR-124 and miR-137 inhibit proliferation of glioblastoma multiforme cells and induce differentiation of brain tumor stem cells. *BMC Med* 2008; **6**: 14.
9 Smrt RD, Szulwach KE, Pfeiffer RL, Li X, Guo W, Pathania M *et al.* MicroRNA miR-137 regulates neuronal maturation by targeting ubiquitin ligase mind Bomb-1. *Stem Cells* 2010; **28**: 1060–1070.
10 Sun G, Ye P, Murai K, Lang M-F, Li S, Zhang H *et al.* miR-137 forms a regulatory loop with nuclear receptor TLX and LSD1 in neural stem cells. *Nat Commun* 2011; **2**: 529.
11 Szulwach KE, Li X, Smrt RD, Li Y, Luo Y, Lin L *et al.* Cross talk between microRNA and epigenetic regulation in adult neurogenesis. *J Cell Biol* 2010; **189**: 127–141.
12 O'Reilly KC, Kao H-Y, Lee H, Fenton AA. Converging on a core cognitive deficit: the impact of various neurodevelopmental insults on cognitive control. *Front Neurosci* 2014; **8**: 153.
13 Toro C, Deakin J. Adult neurogenesis and schizophrenia: a window on abnormal early brain development? *Schizophr Res* 2007; **90**: 1–14.
14 Collins AL, Kim Y, Bloom RJ, Kelada SN, Sethupathy P, Sullivan PF. Transcriptional targets of the schizophrenia risk gene MIR137. *Transl Psychiatry* 2014; **4**: e404.
15 Hill MJ, Donocik JG, Nuamah RA, Mein CA, Sainz-Fuertes R, Bray NJ. Transcriptional consequences of schizophrenia candidate miR-137 manipulation in human neural progenitor cells. *Schizophr Res* 2014; **153**: 225–230.
16 Wright C, Turner JA, Calhoun VD, Perrone-Bizzozero N. Potential impact of miR-137 and its targets in schizophrenia. *Front Genet* 2013; **4**: 58.
17 Vita A, De Peri L, Deste G, Sacchetti E. Progressive loss of cortical gray matter in schizophrenia: a meta-analysis and meta-regression of longitudinal MRI studies. *Transl Psychiatry* 2012; **2**: e190.
18 Hariri AR, Drabant EM, Weinberger DR. Imaging genetics: perspectives from studies of genetically driven variation in serotonin function and corticolimbic affective processing. *Biol Psychiatry* 2006; **59**: 888–897.
19 van Erp TGM, Guella I, Vawter MP, Turner J, Brown GG, McCarthy G *et al.* Schizophrenia miR-137 locus risk genotype is associated with dorsolateral prefrontal cortex hyperactivation. *Biol Psychiatry* 2014; **75**: 398–405.
20 Mothersill O, Morris DW, Kelly S, Rose EJ, Fahey C, O'Brien C *et al.* Effects of MIR137 on fronto-amygdala functional connectivity. *NeuroImage* 2014; **90**: 189–195.
21 Liu B, Zhang X, Hou B, Li J, Qiu C, Qin W *et al.* The impact of MIR137 on dorsolateral prefrontal–hippocampal functional connectivity in healthy subjects. *Neuropsychopharmacology* 2014; **39**: 2153–2160.
22 Lett TA, Chakavarty MM, Felsky D, Brandl EJ, Tiwari AK, Gon\ccalves VF *et al.* The genome-wide supported microRNA-137 variant predicts phenotypic heterogeneity within schizophrenia. *Mol Psychiatry* 2013; **18**: 443–450.
23 Kelly S, Morris DW, Mothersill O, Rose EJ, Fahey C, O'Brien C *et al.* Genome-wide schizophrenia variant at MIR137 does not impact white matter microstructure in healthy participants. *Neurosci Lett* 2014; **574**: 6–10.
24 Whalley HC, Papmeyer M, Romaniuk L, Sprooten E, Johnstone EC, Hall J *et al.* Impact of a microRNA MIR137 susceptibility variant on brain function in people at high genetic risk of schizophrenia or bipolar disorder. *Neuropsychopharmacology* 2012; **37**: 2720–2729.
25 Cousijn H, Eissing M, Fernández G, Fisher SE, Franke B, Zwiers M *et al.* No effect of schizophrenia risk genes MIR137, TCF4, and ZNF804A on macroscopic brain structure. *Schizophr Res* 2014; **159**: 329–332.
26 Patel VS, Kelly S, Wright C, Gupta CN, Arias-Vasquez A, Perrone-Bizzozero N *et al.* MIR137HG risk variant rs1625579 genotype is related to corpus callosum volume in schizophrenia. *Neurosci Lett* 2015; **602**: 44–49.
27 Kuswanto CN, Sum MY, Qiu A, Sitoh Y-Y, Liu J, Sim K. The impact of genome wide supported microRNA-137 (MIR137) risk variants on frontal and striatal white matter integrity, neurocognitive functioning, and negative symptoms in schizophrenia. *Am J Med Genet B Neuropsychiatr Genet* 2015; **168B**: 317–326.
28 International Schizophrenia C, Purcell SM, Wray NR, Stone JL, Visscher PM, O'Donovan MC *et al.* Common polygenic variation contributes to risk of schizophrenia and bipolar disorder. *Nature* 2009; **460**: 748–752.
29 Wright C, Calhoun VD, Ehrlich S, Wang L, Turner JA, Perrone-Bizzozero NI. Meta gene set enrichment analyses link miR-137-regulated pathways with schizophrenia risk. *Front Genet* 2015; **6**: 147.
30 Chen L, Wang X, Wang H, Li Y, Yan W, Han L *et al.* miR-137 is frequently down-regulated in glioblastoma and is a negative regulator of Cox-2. *Eur J Cancer* 2012; **48**: 3104–3111.
31 Quednow BB, Brzózka MM, Rossner MJ. Transcription factor 4 (TCF4) and schizophrenia: integrating the animal and the human perspective. *Cell Mol Life Sci* 2014; **71**: 2815–2835.
32 Müller N, Krause D, Dehning S, Musil R, Schennach-Wolff R, Obermeier M *et al.* Celecoxib treatment in an early stage of schizophrenia: results of a randomized, double-blind, placebo-controlled trial of celecoxib augmentation of amisulpride treatment. *Schizophr Res* 2010; **121**: 118–124.
33 Tang B, Capitao C, Dean B, Thomas EA. Differential age- and disease-related effects on the expression of genes related to the arachidonic acid signaling pathway in schizophrenia. *Psychiatry Res* 2012; **196**: 201–206.
34 Yuan P, Zhou R, Wang Y, Li X, Li J, Chen G *et al.* Altered levels of extracellular signal-regulated kinase signaling proteins in postmortem frontal cortex of individuals with mood disorders and schizophrenia. *J Affect Disord* 2010; **124**: 164–169.
35 Chen Q, Chen X, Zhang M, Fan Q, Luo S, Cao X. miR-137 is frequently down-regulated in gastric cancer and is a negative regulator of Cdc42. *Dig Dis Sci* 2011; **56**: 2009–2016.
36 Liang L, Li X, Zhang X, Lv Z, He G, Zhao W *et al.* MicroRNA-137, an HMGA1 Target, suppresses colorectal cancer cell invasion and metastasis in mice by directly targeting FMNL2. *Gastroenterology* 2013; **144**: 624–635.e4.
37 Zhu X, Li Y, Shen H, Li H, Long L, Hui L *et al.* miR-137 inhibits the proliferation of lung cancer cells by targeting Cdc42 and Cdk6. *FEBS Lett* 2013; **587**: 73–81.
38 Taurin S, Sandbo N, Yau DM, Sethakorn N, Dulin NO. Phosphorylation of -catenin by PKA promotes ATP-induced proliferation of vascular smooth muscle cells. *AJP Cell Physiol* 2008; **294**: C1169–C1174.
39 Hino S-i, Tanji C, Nakayama KI, Kikuchi A. Phosphorylation of -catenin by cyclic AMP-dependent protein kinase stabilizes -catenin through inhibition of its ubiquitination. *Mol Cell Biol* 2005; **25**: 9063–9072.
40 Tamura M, Sebastian S, Yang S, Gurates B, Fang Z, Bulun SE. Interleukin-1β elevates cyclooxygenase-2 protein level and enzyme activity via increasing its mRNA stability in human endometrial stromal cells: an effect mediated by extracellularly regulated kinases 1 and 2. *J Clin Endocrinol Metab* 2002; **87**: 3263–3273.
41 He Q, Harding P. LaPointe MC. PKA, Rap1, ERK1/2, and p90RSK mediate PGE2 and EP4 signaling in neonatal ventricular myocytes. *AJP Heart Circ Physiol* 2010; **298**: H136–H143.
42 Chen J, Liu J, Calhoun VD, Arias-Vasquez A, Zwiers MP, Gupta CN *et al.* Exploration of scanning effects in multi-site structural MRI studies. *J Neurosci Methods* 2014; **230**: 37–50.
43 Turner JA, Calhoun VD, Michael A, van Erp TGM, Ehrlich S, Segall JM *et al.* Heritability of multivariate gray matter measures in schizophrenia. *Twin Res Hum Genet* 2012; **15**: 324–335.
44 Xu L, Groth KM, Pearlson G, Schretlen DJ, Calhoun VD. Source-based morphometry: the use of independent component analysis to identify gray matter differences with application to schizophrenia. *Hum Brain Mapp* 2009; **30**: 711–724.
45 Gupta CN, Chen J, Liu J, Damaraju E, Wright C, Perrone-Bizzozero NI *et al.* Genetic markers of white matter integrity in schizophrenia revealed by parallel ICA. *Front Hum Neurosci* 2015; **9**: 100.
46 Gollub RL, Shoemaker JM, King MD, White T, Ehrlich S, Sponheim SR *et al.* The MCIC collection: a shared repository of multi-modal, multi-site brain image data from a clinical investigation of schizophrenia. *Neuroinformatics* 2013; **11**: 367–388.
47 Wang L, Kogan A, Cobia D, Alpert K, Kolasny A, Miller MI *et al.* Northwestern University schizophrenia data and software tool (NUSDAST). *Front Neuroinformatics* 2013; **7**: 25.
48 Walton E, Turner J, Gollub RL, Manoach DS, Yendiki A, Ho B-C *et al.* Cumulative genetic risk and prefrontal activity in patients with schizophrenia. *Schizophr Bull* 2012; **39**: 703–711.
49 Ashburner J, Friston KJ. Unified segmentation. *NeuroImage* 2005; **26**: 839–851.
50 Gupta CN, Calhoun VD, Rachakonda S, Chen J, Patel V, Liu J *et al.* Patterns of gray matter abnormalities in schizophrenia based on an international mega-analysis. *Schizophr Bull* 2014; **41**: 1133–1142.
51 Chen J, Calhoun VD, Pearlson GD, Perrone-Bizzozero N, Sui J. Guided exploration of genomic risk for gray matter abnormalties in schizophrenia using parallel independent component analysis with reference. *NeuroImage* 2013; **83**: 384–396.

52 Rissanen J. Modeling by shortest data description. *Automatica* 1978; **14**: 465–471.
53 Faul F, Erdfelder E, Lang A-G, Buchner A. G* Power 3: a flexible statistical power analysis program for the social, behavioral, and biomedical sciences. *Behav Res Methods* 2007; **39**: 175–191.
54 Faul F, Erdfelder E, Buchner A, Lang A-G. Statistical power analyses using G*Power 3.1: tests for correlation and regression analyses. *Behav Res Methods* 2009; **41**: 1149–1160.
55 D'agostino RB, Belanger A Jr, RBD. A. Suggestion for using powerful and informative tests of normality. *Am Stat* 1990; **44**: 316–321.
56 Kalueff AV, Poudel MK, Stewart AM. Hidden heritability and genetic parsing of complex CNS disorders. *Stress Brain Behav* 2015; **3**: 1–2.
57 Walton E, Geisler D, Lee PH, Hass J, Turner JA, Liu J *et al.* Prefrontal inefficiency is associated with polygenic risk for schizophrenia. *Schizophr Bull* 2014; **40**: 1263–1271.
58 Hass J, Walton E, Wright C, Beyer A, Scholz M, Turner J *et al.* Associations between DNA methylation and schizophrenia-related intermediate phenotypes — a gene set enrichment analysis. *Prog Neuropsychopharmacol Biol Psychiatry* 2015; **59**: 31–39.
59 Qiu L, Tian L, Pan C, Zhu R, Liu Q, Yan J *et al.* Neuroanatomical circuitry associated with exploratory eye movement in schizophrenia: a voxel-based morphometric study. *PLoS One* 2011; **6**: e25805.
60 Guo S, Kendrick KM, Yu R, Wang H-LS, Feng J. Key functional circuitry altered in schizophrenia involves parietal regions associated with sense of self: key functional circuitry altered in schizophrenia. *Hum Brain Mapp* 2014; **35**: 123–139.
61 Curcic-Blake B, Liemburg E, Vercammen A, Swart M, Knegtering H, Bruggeman R *et al.* When Broca goes uninformed: reduced information flow to Broca's area in schizophrenia patients with auditory hallucinations. *Schizophr Bull* 2013; **39**: 1087–1095.
62 Chen Y-H, Edgar JC, Huang M, Hunter MA, Epstein E, Howell B *et al.* Frontal and superior temporal auditory processing abnormalities in schizophrenia. *NeuroImage Clin* 2013; **2**: 695–702.
63 Diederen KMJ, Daalman K, de Weijer AD, Neggers SFW, van Gastel W, Blom JD *et al.* Auditory hallucinations elicit similar brain activation in psychotic and nonpsychotic individuals. *Schizophr Bull* 2012; **38**: 1074–1082.
64 Sommer IE, Clos M, Meijering AL, Diederen KM, Eickhoff SB. Resting state functional connectivity in patients with chronic hallucinations. *PLoS One* 2012; **7**: e43516.
65 Becerril KE, Barch DM. Conflict and error processing in an extended cingulo-opercular and cerebellar network in schizophrenia. *NeuroImage Clin* 2013; **3**: 470–480.
66 Thimm M, Kircher T, Kellermann T, Markov V, Krach S, Jansen A *et al.* Effects of a CACNA1C genotype on attention networks in healthy individuals. *Psychol Med* 2011; **41**: 1551–1561.
67 Huang M-X, Lee RR, Gaa KM, Song T, Harrington DL, Loh C *et al.* Somatosensory system deficits in schizophrenia revealed by MEG during a median-nerve oddball task. *Brain Topogr* 2010; **23**: 82–104.
68 Martinez A, Hillyard SA, Dias EC, Hagler DJ, Butler PD, Guilfoyle DN *et al.* Magnocellular pathway impairment in schizophrenia: evidence from functional magnetic resonance imaging. *J Neurosci* 2008; **28**: 7492–7500.
69 Cancedda L, Putignano E, Impey S, Maffei L, Ratto GM, Pizzorusso T. Patterned vision causes CRE-mediated gene expression in the visual cortex through PKA and ERK. *J Neurosci* 2003; **23**: 7012–7020.
70 Bhojraj TS, Francis AN, Montrose DM, Keshavan MS. Grey matter and cognitive deficits in young relatives of schizophrenia patients. *NeuroImage* 2011; **54**: S287–S292.
71 Sellier C, Hwang VJ, Dandekar R, Durbin-Johnson B, Charlet-Berguerand N, Ander BP *et al.* Decreased DGCR8 expression and miRNA dysregulation in individuals with 22q11. 2 deletion syndrome. *PloS One* 2014; **9**: e103884.
72 Kates WR, Bansal R, Fremont W, Antshel KM, Hao X, Higgins AM *et al.* Mapping cortical morphology in youth with velocardiofacial (22q11. 2 deletion) syndrome. *J Am Acad Child Adolesc Psychiatry* 2011; **50**: 272–282.
73 Siegert S, Seo J, Kwon EJ, Rudenko A, Cho S, Wang W *et al.* The schizophrenia risk gene product miR-137 alters presynaptic plasticity. *Nat Neurosci* 2015; **18**: 1008–1016.
74 Funk AJ, McCullumsmith RE, Haroutunian V, Meador-Woodruff JH. Abnormal activity of the MAPK-and cAMP-associated signaling pathways in frontal cortical areas in postmortem brain in schizophrenia. *Neuropsychopharmacology* 2012; **37**: 896–905.

Supplementary Information accompanies the paper on the Translational Psychiatry website (http://www.nature.com/tp)